

Improved field uniformity in EMC chamber for 6G communication

Eugene Rhee, Junhee Cho

Department of Electronic Engineering, College of Engineering, Sangmyung University, Cheonan, Republic of Korea

Article Info

Article history:

Received Mar 6, 2023

Revised Jul 7, 2023

Accepted Jul 16, 2023

Keywords:

6G

Chamber

Diffuser

Electromagnetic compatibility

FDTD

ABSTRACT

This paper shows electromagnetic field uniformity in an electromagnetic compatibility (EMC) chamber that is used as a test facility for measuring electromagnetic interference and radiated immunity of 6G communication systems. While not defined yet, 6G radio frequency will work in the wavelength ranges above 95 GHz. With this reason, this paper designed a schroeder-type quadratic residue diffuser for 95 GHz to generate a uniform electromagnetic field in the EMC chamber and studied the field uniformity characteristics in it. To analyze the distribution of electromagnetic fields inside the EMC chamber, finite-difference time-domain (FDTD) numerical analysis method is used. The simulation results show that the EMC chamber with this diffuser satisfies the requirements of international standards and has improved the field uniformity in the chamber.

This is an open access article under the [CC BY-SA](https://creativecommons.org/licenses/by-sa/4.0/) license.



Corresponding Author:

Junhee Cho

Department of Electronic Engineering, College of Engineering, Sangmyung University

Cheonan, Republic of Korea

Email: jh_cho@smu.ac.kr

1. INTRODUCTION

The future of 6G communication envisions an intelligent communication infrastructure that can connect virtual and physical realities without the constraints of time and space. This will be achieved by leveraging advancements in 5G communication performance, network intelligence, and communication coverage. To realize this vision, 6G communication will require technology characteristics such as hyperspace, ultra-intelligence, and supernova, in addition to expanding on 5G's requirements for ultra-high speed, ultra-low delay, and ultra-connectedness. While 5G communication services focused on performance requirements, the requirements for 6G communication services can be categorized into three areas: performance, structure, and reliability. For example, the maximum speed for 6G communication could reach up to 1,000 Gbps with a wireless delay of 100 microseconds. This would be 50 times faster than 5G communication, and the wireless delay would be reduced to 1/10th of that of 5G communication [1]–[3]. Advanced countries and companies worldwide are actively researching nine key technologies, including Tbps wireless communication, 3D mobile communication, intelligent wireless access, THz RF components, THz frequency, Tbps optical communication, 3D satellite communication, end-to-end ultra-precision networks, and intelligent mobile core networks. Among these technologies, the field of three-dimensional spatial mobile communication, which includes urban air mobility (UAM) and unmanned aerial vehicles (UAVs), is a new industry that has significant potential in the public sector. Therefore, comprehensive government-led efforts are required to facilitate its adoption. In addition to the development of Tbps-class super-performance communication technology, THz frequency research requires government policy support for frequency permission testing, frequency distribution and allocation, and safety research for research purposes [4]. In the network sector, government support is needed for industry-academic cooperation R&D to secure differentiated intellectual property rights

(IPR) and enhance the competitiveness of industries. 6G communication is expected to implement a super-intelligent network that can operate autonomously and provide future intelligence services by applying artificial intelligence to the entire communication network. If commercialized, the ambient internet of everything (AIoE) which connects all environments beyond the internet of things (IoT) is also expected to become a reality. In preparation for this, the international electrotechnical commission (IEC) is developing a 6G mobile communication measurement standard. The IEC is working on establishing a measurement standard that can utilize the 6G frequency band, which covers more than 95-150 GHz and up to 300 GHz without issues.

Electromagnetic compatibility (EMC) is a branch of electrical science that focuses on reducing the level of unwanted electromagnetic energy, known as electromagnetic interference (EMI), generated and propagated by electrical and electronic devices to an appropriate level. The suppression of electromagnetic disturbances to improve EMC is achieved through two methods: suppressing the emission of unwanted waves and reducing the sensitivity of electronic devices to unwanted waves. Devices that generate unwanted waves are called sources, while devices that are interfered with by unwanted waves are called victims or equipment under test (EUT) [5], [6]. To ensure EMC, methods such as suppressing unwanted waves of a source, increasing resistance in the design of a sensitive product, and reducing sensitivity through electromagnetic wave shielding are used. Recent electrical and electronic devices require higher technology to implement EMC compared to the past. This is because the first part has been digitized, operating at a lower voltage, and the introduction of nonconductive materials such as plastics has reduced the electromagnetic shielding capability of metal instruments in the past, and third, interference due to miniaturization and integration has increased. The international standard for ensuring EMC of electrical and electronic devices is IEC 61,000 established by the TC77 subcommittee of IEC [5], [6]. Many countries around the world operate EMC laws by applying these international standards according to their country's circumstances. This paper researches and analyzes the electromagnetic field uniformity inside the chamber for the EMC test of 6G communication devices and facilities and proposes a schroeder-type quadratic residue diffuser to solve the problem of the existing EMC chamber and to improve the field uniformity in it.

2. EMC CHAMBER

Figures 1 and 2 briefly show the difference between SAC and EMC chamber. Unlike SAC, EMC chambers that use two stirrers have a wider measurement space because they do not attach an absorber to the wall and do not require periodic maintenance of the absorber. However, EMC chamber's stirrer is also a bulky facility, so it occupies a certain space in EMC chamber [7], [8], and the maintenance cost of the step motor required to rotate the stirrer is also considerable [9], [10]. This paper proposes schroeder-type quadratic residue diffuser instead of EMC chamber stirrer to solve these problems as shown in Figure 3. Because the diffuser is small in size and can be easily attached to the wall, it does not occupy much space in the EMC chamber than the stirrer and does not incur maintenance costs because it is a fixture rather than a rotating body.

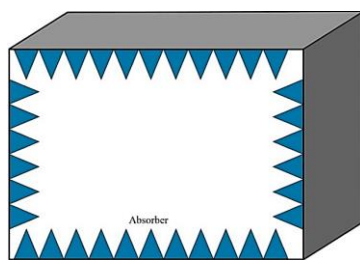


Figure 1. Semi-anechoic chamber with absorbers

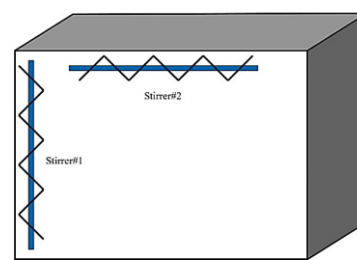


Figure 2. Typical EMC chamber with two stirrers

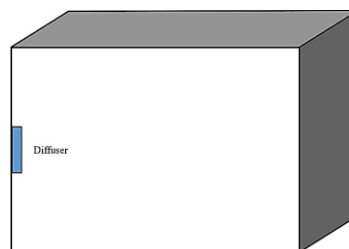


Figure 3. Proposed EMC chamber with schroeder quadratic residue diffuser

3. SCHROEDER QUADRATIC RESIDUE DIFFUSER

As mentioned above, this paper proposes to apply the schroeder quadratic residue diffuser to the EMC chamber instead of the existing stirrer to secure a wider measurement space within the EMC chamber, ease of installation of the device, and reduced maintenance costs. The (1) is a quadratic residue method to obtain a residue. Here, n is an integer from zero to $(N-1)$, γ is a maximum integer satisfying $0 \leq n^2 - \gamma N$, and N is a prime number. This sequence repeats N random numbers with N cycles [11]. This means that schroeder quadratic residue diffuser is always configured in a symmetrical shape. Therefore, in order to construct a more random form, this paper designs schroeder quadratic residue diffuser by (2). The result of (2) creates an asymmetric residue value and forms a more random form compared to (1) [11].

$$S_n = |n^2 - \gamma N| \tag{1}$$

$$S_c = |n^3 - \gamma N| \tag{2}$$

The structure of schroeder quadratic residue diffuser is determined according to the range of frequencies to be used, and in this study, a schroeder quadratic residue diffuser with a frequency range of 95 GHz was designed in consideration of the test frequency to be numerically analyzed. In a schroeder quadratic residue diffuser, the width of the well w is determined by λ_{\max} (f_{\max}) and the depth d_n by λ_{\min} (f_{\min}) [11]. Figure 4 shows the shape of the schroeder quadratic residue diffuser designed for one cycle of the depth of the diffuser.

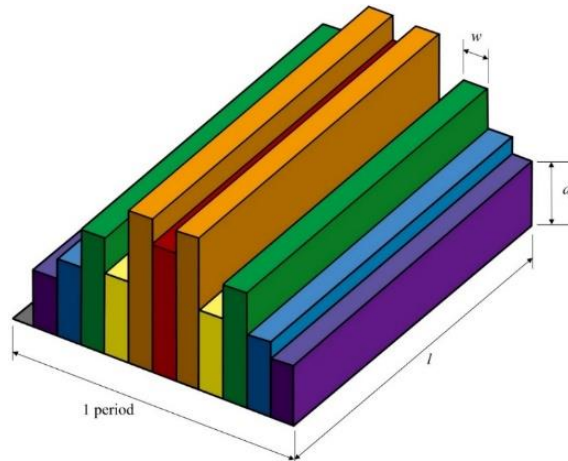


Figure 4. Schroeder quadratic residue diffuser for 95 GHz

4. FDTD SIMULATION

Basically, the finite-difference time-domain (FDTD) method utilizes two finite difference equations modified by applying the maxwell differential equations to the space and time regions with a central difference method. In (3) and (4), the time differential operator $\frac{\partial}{\partial t}$ and the space differential operator $\frac{\partial}{\partial u}$ (where u is x , y , and z) are approximated as (5) because they both use the central difference method.

$$\nabla \times \vec{H} = \epsilon \frac{\partial \vec{E}}{\partial t} \tag{3}$$

$$\nabla \times \vec{E} = \mu \frac{\partial \vec{H}}{\partial t} \tag{4}$$

$$\frac{\partial}{\partial u} \cong \tilde{\partial}_u = \frac{1}{\Delta u} (s_u^+ - s_u^-) \tag{5}$$

Where s_u^+ and s_u^- are movement operators defined as following (6) and (7).

$$s_u^+ F(u, v, \dots) = F\left(u + \frac{\Delta u}{2}, v, \dots\right) \tag{6}$$

$$s_u^- F(u, v, \dots) = F\left(u - \frac{\Delta u}{2}, v, \dots\right) \quad (7)$$

In the FDTD algorithm, the electric field and the magnetic field are updated every hour. On the other hand, the FDTD calculation has numerical variance characteristics because it was discretized by the central difference approximation. In the time and space generated by the central difference approximation, the error has a secondary accuracy that decreases. Therefore, to minimize the numerical variance characteristics, Δx , Δy , and Δz should be less than at least 1/10 of the wavelength at the maximum frequency of the pulse. Meanwhile, since the FDTD algorithm has a positive function form, Δt must satisfy the courant-friedrick-lewy (CFL) stability conditions [12]–[14].

In order to investigate the internal electromagnetic field distribution of the EMC chamber to which the schroeder quadratic residue diffuser was applied, the simulation was performed using the FDTD numerical analysis method. The simulation software was interpreted using remcom's XFDTD simulation tool and the Yee algorithm is applied, using a finite difference equation to interpret the field of electromagnetic field for time and space [15]–[18]. The vector of (3) and (4) can be expressed as six scalar equations in rectangular coordinate system as shown in Figure 5. If each component of the electric field and magnetic field shown in the Yee spatial grid is approximated by a central difference over time and space, ampere's law and Faraday's law can be expressed by discrete equations [18]. The EMC chamber shall have an appropriate size to maintain the multi-mode electromagnetic environment, which is closely related to the lowest usable high frequency (LUF) to satisfy the field uniformity of the EMC chamber. Therefore, the test frequency was set to 95 GHz in consideration of the cutoff frequency and diffuser design, and the size of the Yee cell was set to Δx , Δy , and $\Delta z = 0.01$ m in consideration of the frequency. To satisfy the CFL stability conditions, the discrete time was set to 19.25 ps ($=\Delta t$) and the total number of time intervals was set to 25,000 [19]–[22]. In this paper, the size of the EMC chamber was set to $95\Delta x \times 95\Delta y \times 95\Delta z$, and the source for field generation was set to y -polarity in cells (48, 82, and 48) as a 1 V sinusoidal point source. The EMC chamber was modeled with a perfect electric conductor (PEC) cell, and the diffuser medium and external boundary conditions were also set to PEC [23]–[27]. The schroeder quadratic residue diffuser was applied to the center of the start ($y=0$) portion of the x - z plane inside the EMC chamber. To investigate the field distribution, a total of 80 test points, 16 per plane, were set on five test planes of the test volume, and the test space was determined by considering the definition of EMC chamber described in IEC 61,000-4-3 [5].

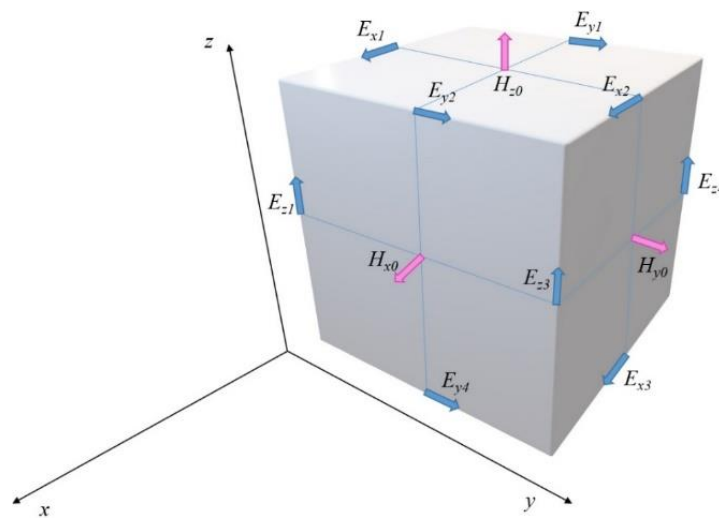


Figure 5. Yee cell

5. RESULTS AND DISCUSSIONS

For the analysis of the simulation results, data on the electric field intensity were extracted using MATLAB, and numerical analysis and statistical approaches were performed. When schroeder quadratic diffuser is applied to the EMC chamber, the result of the simulated electric field intensity distribution for the x - z plane at $y=48$ is shown in Figures 6 and 7. To analyze the effectiveness of the designed diffuser, the distribution of electric field strength within the EMC chamber to which the diffuser is applied and the EMC chamber to which diffuser is not applied was compared.

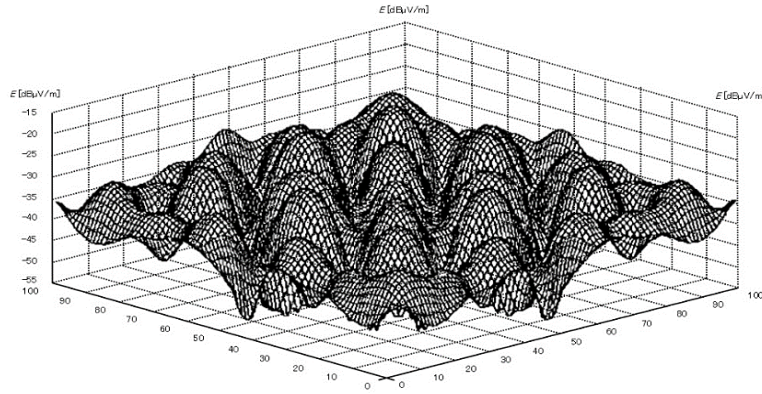


Figure 6. Electric field intensity distribution of EMC chamber without diffuser

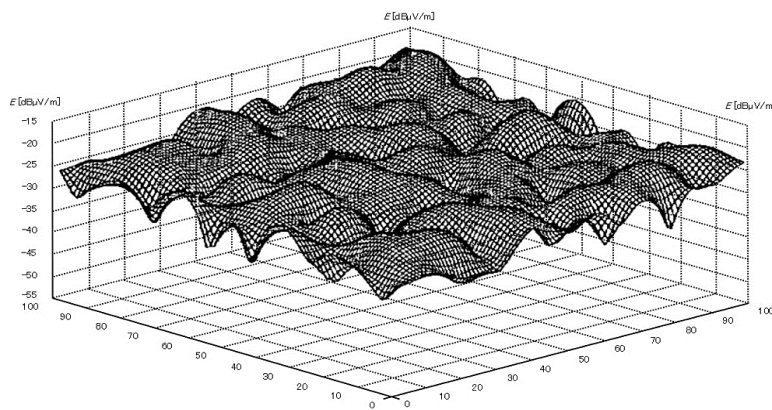


Figure 7. Electric field intensity distribution of EMC chamber with diffuser

At the distribution shape of the electric field intensity in Figure 7, it can be seen that the difference in height of the distribution valley in the EMC chamber to which the diffuser is applied is reduced. This means that the field uniformity is improved. Using the numerical analysis results when schroeder quadratic diffuser is applied, the average value, standard deviation, maximum value, minimum value, and tolerance results for 60 samples which are 75 % of the 80 field strength values in the test space shown in Figures 6 and 7 are as shown in Table 1. As shown in Figure 7 and Table 1, it can be seen that the uniformity of the field was improved when schroeder quadratic diffuser was attached to the same source, and the result satisfies the field uniformity within ± 6 dB required by IEC 61,000 international standards [4], [5].

Table 1. Electric field intensity (75% sampling)

E [dBuV/m]	Without diffuser	With diffuser
Mean	-45.48	-29.13
Standard deviation	9.16	2.79
Maximum	-54.64	-31.92
Minimum	-36.32	-26.34
Tolerance [dB]	18.32	5.58

6. CONCLUSION

As a result of designing and simulating a Schroeder quadratic diffuser capable of spreading electromagnetic waves in a frequency 95 GHz band that is expected to deteriorate due to 6G mobile communication, mobile internet, and wireless local area network (LAN), which is preparing for commercialization, and also improved power efficiency. The biggest issue in this paper is whether EMC chamber to which the designed schroeder quadratic residue diffuser is applied has the same field uniformity as EMC chamber to which the stirrer is applied. It was confirmed that the applied schroeder quadratic residue diffuser showed field uniformity within ± 6 dB tolerance, and the standard deviation characteristics were excellent at one or less, thereby satisfying IEC 61,000 international standards.

ACKNOWLEDGEMENTS

This research was funded by a 2022 research grant from Sangmyung University (2022-A000-0003).




REFERENCES

- [1] I. Abubakar, J. Din, M. Alhilali, and H. Y. Lam, "Interference and electromagnetic compatibility challenges in 5G wireless network deployments," *Indonesian Journal of Electrical Engineering and Computer Science (IJECS)*, vol. 5, no. 3, pp. 612–621, Mar. 2017, doi: 10.11591/ijeecs.v5.i3.pp612-621.
- [2] B. Djamel, H. Houassine, N. Kabache, and D. Moussaoui, "Electromagnetic nonlinear parametric study of the SynRM using FEM method," *Indonesian Journal of Electrical Engineering and Computer Science (IJECS)*, vol. 24, no. 2, pp. 637–648, Nov. 2021, doi: 10.11591/ijeecs.v24.i2.pp637-648.
- [3] T. Baba, N. A. C. Mustapha, and N. F. Hasbullah, "A review on techniques and modelling methodologies used for checking electromagnetic interference in integrated circuits," *Indonesian Journal of Electrical Engineering and Computer Science (IJECS)*, vol. 25, no. 2, pp. 796–804, Feb. 2022, doi: 10.11591/ijeecs.v25.i2.pp796-804.
- [4] A. H. P. Mohammadi, M. C. Amirani, and Faghihi, "Comparison of shielding effectiveness in complex curved structure with different numerical methods, FDTD, MOM and equivalent circuit," *Indonesian Journal of Electrical Engineering and Computer Science (IJECS)*, vol. 12, no. 3, pp. 1010–1019, Dec. 2018, doi: 10.11591/ijeecs.v12.i3.pp1010-1019.
- [5] International Electrotechnical Commission, "IEC61000-4-3 Testing and measurement techniques-radiated, radio-frequency, electromagnetic field immunity test 3rd ed." USA.
- [6] Electromagnetic Compatibility, "Part 4-21: Testing and measurement techniques-reverberation chamber test methods." Standard IEC, 2011.
- [7] G. Andrieu, N. Ticaud, and F. Lescoat, "On the risk to declare EMC compliant a faulty EUT during radiated susceptibility tests in reverberation chambers," *IEEE Transactions on Electromagnetic Compatibility*, vol. 62, no. 3, pp. 645–653, Jun. 2020, doi: 10.1109/TEMC.2019.2919247.
- [8] A. De Leo, G. Cerri, P. Russo, and V. M. Primiani, "A novel emission test method for multiple monopole source stirred reverberation chambers," *IEEE Transactions on Electromagnetic Compatibility*, vol. 62, no. 5, pp. 2334–2337, Oct. 2020, doi: 10.1109/TEMC.2020.2999651.
- [9] L. Cappetta, M. Feo, V. Fiumara, V. Pierro, and I. M. Pinto, "Electromagnetic chaos in mode-stirred reverberation enclosures," *IEEE Transactions on Electromagnetic Compatibility*, vol. 40, no. 3, pp. 185–192, 1998, doi: 10.1109/15.709415.
- [10] A. Gifuni, L. Bastianelli, M. Migliaccio, F. Moglie, V. M. Primiani, and G. Gradoni, "On the estimated measurement uncertainty of the insertion loss in a reverberation chamber including frequency stirring," *IEEE Transactions on Electromagnetic Compatibility*, vol. 61, no. 5, pp. 1414–1422, Oct. 2019, doi: 10.1109/TEMC.2018.2870073.
- [11] M. Mehta, J. Johnson, and J. Rocafort, "Architectural principles and design," TRID: Englewood Cliffs, 1999.
- [12] R. J. Luebbers, K. S. Kunz, M. Schneider, and F. Hunsberger, "A finite-difference time-domain near zone to far zone transformation," *IEEE Transactions on Antennas and Propagation*, vol. 39, no. 4, pp. 429–433, Apr. 1991, doi: 10.1109/8.81453.
- [13] J. B. Cole, "A high accuracy FDTD algorithm to solve microwave propagation and scattering problems on a coarse grid," *IEEE Transactions on Microwave Theory and Techniques*, vol. 43, no. 9, pp. 2053–2058, 1995, doi: 10.1109/22.414540.
- [14] G. Mur, "Absorbing Boundary Conditions for the finite-difference approximation of the time-domain electromagnetic-field equations," *IEEE Transactions on Electromagnetic Compatibility*, vol. EMC-23, no. 4, pp. 377–382, Nov. 1981, doi: 10.1109/TEMC.1981.303970.
- [15] X. Zhang, J. Fang, K. K. Mei, and Y. Liu, "Calculations of the dispersive characteristics of microstrips by the time-domain finite difference method," *IEEE Transactions on Microwave Theory and Techniques*, vol. 36, no. 2, pp. 263–267, 1988, doi: 10.1109/22.3514.
- [16] R. Luebbers, F. R. Hunsberger, K. S. Kunz, R. B. Standler, and M. Schneider, "A frequency-dependent finite-difference time-domain formulation for dispersive materials," *IEEE Transactions on Electromagnetic Compatibility*, vol. 32, no. 3, pp. 222–227, 1990, doi: 10.1109/15.57116.
- [17] J. J. Simpson and A. Taflove, "Three-dimensional FDTD modeling of impulsive ELF propagation about the earth-sphere," *IEEE Transactions on Antennas and Propagation*, vol. 52, no. 2, pp. 443–451, Feb. 2004, doi: 10.1109/TAP.2004.823953.
- [18] H. D. Raedt, K. Michielsen, J. S. Kole, and M. T. Figge, "Solving the maxwell equations by the chebyshev method: a one-step finite-difference time-domain algorithm," *IEEE Transactions on Antennas and Propagation*, vol. 51, no. 11, pp. 3155–3160, Nov. 2003, doi: 10.1109/TAP.2003.818809.
- [19] L. R. Arnaut, "Statistics of the quality factor of a rectangular reverberation chamber," *IEEE Transactions on Electromagnetic Compatibility*, vol. 45, no. 1, pp. 61–76, Feb. 2003, doi: 10.1109/TEMC.2002.808021.
- [20] K. Umashankar and A. Taflove, "A novel method to analyze electromagnetic scattering of complex objects," *IEEE Transactions on Electromagnetic Compatibility*, vol. EMC-24, no. 4, pp. 397–405, Nov. 1982, doi: 10.1109/TEMC.1982.304054.
- [21] A. Taflove, "Application of the finite-difference time-domain method to sinusoidal steady-state electromagnetic-penetration problems," *IEEE Transactions on Electromagnetic Compatibility*, vol. EMC-22, no. 3, pp. 191–202, Aug. 1980, doi: 10.1109/TEMC.1980.303879.
- [22] S. Liu, T. Onishi, M. Taki, and S. Watanabe, "Radio frequency electromagnetic field exposure compliance assessments of smart surfaces: two approximate approaches," *IEEE Transactions on Electromagnetic Compatibility*, vol. 64, no. 4, pp. 963–974, Aug. 2022, doi: 10.1109/TEMC.2022.3171044.
- [23] G. A. Kriegsmann, A. Taflove, and K. R. Umashankar, "New formulation of electromagnetic wave scattering using an on-surface radiation boundary condition approach," *IEEE Transactions on Antennas and Propagation*, vol. AP-35, no. 2, pp. 153–161, Feb. 1987, doi: 10.1109/tap.1987.1144062.
- [24] A. S. Nagra and R. A. York, "FDTD analysis of wave propagation in nonlinear absorbing and gain media," *IEEE Transactions on Antennas and Propagation*, vol. 46, no. 3, pp. 334–340, Mar. 1998, doi: 10.1109/8.662652.
- [25] W. Sui, D. A. Christensen, and C. H. Durney, "Extending the two-dimensional FDTD method to hybrid electromagnetic systems with active and passive lumped elements," *IEEE Transactions on Microwave Theory and Techniques*, vol. 40, no. 4, pp. 724–730, Apr. 1992, doi: 10.1109/22.127522.
- [26] E. A. Forgy and W. C. Chew, "A time-domain method with isotropic dispersion and increased stability on an overlapped lattice," *IEEE Transactions on Antennas and Propagation*, vol. 50, no. 7, pp. 983–996, Jul. 2002, doi: 10.1109/TAP.2002.801373.




- [27] J. Wu, Q. Guo, C. Yue, L. Xie, and C. Zhang, "Special electromagnetic interference in the ionosphere directly correlated with power system," *IEEE Transactions on Electromagnetic Compatibility*, vol. 62, no. 3, pp. 947–954, Jun. 2020, doi: 10.1109/TEMC.2019.2918280.

BIOGRAPHIES OF AUTHORS



Eugene Rhee    received the Ph.D. degree in electronics from Hanyang University, Korea, in 2010. He was a visiting professor at Chuo University, Japan from 2010 to 2011. Since 2012, he has been with Sangmyung University, Korea, where he is currently an associate professor in the Department of Electronic Engineering. His research area includes microwave, electromagnetic compatibility, electromagnetic interference, and reverberation chamber. He can be contacted at email: eugenerhee@smu.ac.kr.



Junhee Cho    received his Ph.D. degree in electrical engineering from University of Cambridge, U.K. in 2017. Since 2020, he has been an Assistant Professor in the department of electronics engineering, Sangmyung University, Republic of Korea. His current research interests include nanophotonics-based secure communications. He can be contacted at email: jh_cho@smu.ac.kr.